Applied Nanoscience (2022) 12:1101–1111
https://doi.org/10.1007/s13204-021-01790-y

ORIGINAL ARTICLE

Structural properties and adsorption of uranyl ions on the nanocomposite hydroxyapatite/white clay

E. Broda[1] · A. Gładysz-Płaska[1] · E. Skwarek[1] · V. V. Payentko[2]

Received: 31 December 2020 / Accepted: 6 March 2021 / Published online: 18 March 2021

Abstract

Uranium is more and more extensively applied as a source of energy and can be potentially used for nuclear weapon production. Owing to that fact, the problem of uranium expansion in the environment is the object of research and draw attention many scientists. One of the most effective methods of uranium removal from the wastewater (where uranium is present in a low concentration and occurs mainly in the form of uranyl ion, UO_2^{2+}) is the adsorbent usage. It is important to discover an adsorbent which will be effective, widely available and cheap. The paper discusses properties and the ability of *U* (VI) adsorption on a clay and nanocomposite clay/Hap (hydroxyapatite) obtained by wet method. The adsorbents were characterized by the mentioned below tests: XRD, XRF, the porosity (nitrogen adsorption–desorption method), zeta potential, surface charge density and sorption of *U* (VI). It was shown that nanocrystalline composites Hap/white clay can be appropriate adsorbent for removal of uranyl ions. The adsorption depends on the temperature and pH of the solution.

Keywords Nanocomposite hydroxyapatite/white clay · Uranyl ions · Adsorption

Introduction

Uranium is silvery-white, ductile and slightly paramagnetic metal. It is also the heaviest naturally occurring element, slightly softer than steel. In the earth crust, it is found at the average concentration 3 mg/kg, in the seawater the concentration amounts to 3 μg/dm^3. Being widely spread in nature, uranium is also present, in trace amounts in food and drinking water. (Bleise et al. 2003) Because of increasing usage for both civil and military aspects, the concentration of this element should be monitored and controlled. Uranium can have a significant impact on human health.

Radiotoxicity of uranium is less dangerous than other radioelements due to the emitting of alpha particles with a small penetration ability. The danger occurs when uranium compounds are ingested or inhaled. The chemical toxicity of uranium has been considered to be public health concerns.

In the human organism Uranium usually occurs as a uranyl ion UO_2^{2+} complex. Tetravalent uranium is oxidized to the hexavalent form and next converted to the uranyl ion. (Keith et al. 2007). When dissolved in the acidic system, the uranyl ion is present in free ion form. However, in the neutral or basic system the uranyl ion can form uranyl–hydroxyl or uranyl–carbonate ion pairs (Zhu and Ryan 2018). A large amount of uranium compound in the human body can lead to kidney failure. (Aly and Hamza 2012) Owing to growing usage of uranium and awareness of potential dangers connected with it, efficient methods of protection the environment should be developed. The option to remove uranium is for example anion exchange, reverse osmosis, coagulation, lime softening and the application of adsorbents (Katsoyaiannis and Zouboulis 2013). Uranium adsorption was already tested on hydroxyapatite (Skwarek et al. 2019; Shi et al. 2020) and different kinds of clay minerals (Bachmaf and Merkel 2011). The paper is focussed on uranium adsorption on the white clay and hydroxyapatite/white clay nanocomposite synthesized by the hydrothermal method (Broda et al. 2019).

The literature reports some research on the adsorption of the clay and hydroxyapatite composites. The Hap/clay/nanocellulose composite was characterized as an adsorbent of Cd^{2+}, Ni^{2+} from the contaminated water (Hokkanen et al.

✉ E. Skwarek
ewunias@hektor.umcs.lublin.pl

[1] Faculty of Chemistry, Maria Curie-Skłodowska University, Maria Curie-Skłodowska Sq. 3, 20031 Lublin, Poland

[2] Chuiko Institute of Surface Chemistry, 17 General Naumov Street, Kyiv 03164, Ukraine

2018). Another application of the Hap/clay composite can be tetracycline removal from aqueous solutions (Ersan et al. 2015).

Other ionic substances may also affect the adsorption of metal ions (Wiśniewska et al. 2018; Szewczuk-Karpisz et al. 2020; Fijałkowska et al. 2020).

Thus, the hydroxyapatite and clay nanocomposite can be a new kind of adsorbent, which may be applied for uranium ions removal from aqueous solutions. In this study, synthesis of this nanocomposites was described. Some parameters of nanocomposite and pure white clay were tested, including XRD, porosity by the nitrogen adsorption–desorption, zeta potential, surface charge density and sorption of U (VI).

Experimental

Materials and methods

In this study the nanocomposite of white clay and hydroxyapatite was synthesized applying the wet method, as presented in Fig. 1. White clay was purchased from "Mel-OK" (Kyiv, Ukraine), mined in the Azov region. For preparation of the solutions used in the hydroxyapatite synthesis, di-potassium hydrogen phosphate (pure p.a.) from POCH SA and calcium acetate hydrate (pure) from Riedel-de Haën

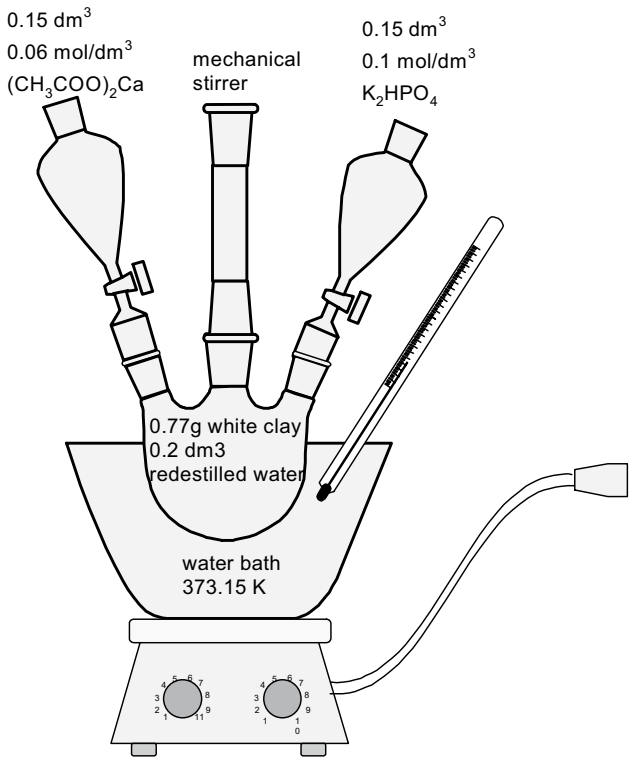

Fig. 1 Diagrammatic drawing synthesis of the hydroxyapatite/white clay nanocomposite

were used. When the solutions were dropwise added into the flask, the suspension was heated for another hour. Then, the obtained nanocomposite was washed with redistilled water, until the value of conductivity of solution over the precipitant was constant. The nanocomposite was dried for 24 h at 80 °C.

The surface of nanocomposite was characterized by X-ray diffraction (XRD). The tests were performed using the diffractometer Empyrean PANalytical with the CULEF HR lamp and the detector-pixcel-3D (active canals 255).

The textural characterization of the spherical activated hydroxyapatite, clay and Hap/clay nanocomposite was based on the nitrogen adsorption–desorption isotherms measured at − 196 °C on the sorptometer ASAP 2405 manufactured by Micrometrics Instrument Corporation. Before the isotherm measurements, the samples were degassed at 50 °C for 8 h. Specific surface area (S_{BET}) of the adsorbents prepared was evaluated in the range of relative pressures (p/p_0) between 0.1 and 0.50, whereas total pore volume (V_t) was calculated by converting the amount of nitrogen adsorbed at a relative pressure of approximately 0.99. Mean pore diameter (d) of the adsorbents prepared was calculated from the equation $d = 4V_t/S_{BET}$.

The properties of the electrical double layer of the nanocomposite were characterized by the potentiometric titration and zeta potential measurements. Titration was carried out at 25 °C under nitrogen atmosphere. The pH value was measured with a set of electrodes: glass REF 451 and calomel pHG201-8. The surface charge density was assigned in dependence of the volume of added acid/base to acquire the same pH value as that of the background electrolyte (0.001 mol/dm^3 $NaNO_3$). The surface charge density was estimated at different uranyl ions concentrations (from 0.001 mol/dm^3 to 0.000001 mol/dm^3). The zeta potential was measured using the Zetasizer Nano-ZS apparatus by Malvern Instruments Ltd.

Influence of uranium adsorption on its percentage content in white clay and nanocomposite Hap/white clay was tested by means of the XRF (*X-Ray Fluorescence Spectroscopy*) method. The apparatus Axios mAX (PANalytical) was used.

The analysis of grain distribution was performed for the white clay, Hap and Hap/white nanocomposite clay by the laser diffraction method using Mastersizer 2000 Malvern Instruments. The tests were done for each adsorbent suspended in 0.001 mol/dm^3 $NaNO_3$ and 0.001 mol/dm^3 $NaNO_3$ with addition of uranyl ions, also at the level 0.001 mol/dm^3. The first measurement was recorded just after preparation of the system. Next, the test was repeated after 3, 48 h and 7 days.

Raw white clay and the Hap/white clay nanocomposite were used as a sorbent in the experiment with U (VI) ion adsorption. A weighed portion of 50 mg was immersed in a mixture with the defined concentration of U(VI) ions

(0.5 mmol/L) and adjusted to the appropriate pH (2.0–10) and constant volume (50 ml). The mixtures were shaken using a mechanical shaker in a temperature-controlled water bath at 25 °C for 4 h with a constant stirring speed of 180 rpm. After equilibration, filtration was carried out, then the solutions were centrifuged. The equilibrium concentration of *U* (VI) was determined by the spectrophotometric method using the Arsenazo indicator (Marczenko and Balcerzak 1998). The measurements were made using a Jasco 6000 spectrophotometer at a wavelength of 655 nm.

The amounts of *U*(VI) adsorbed on the white clay sorbent *(Q)* [mg/g], the %S percentage of uranium removal as well as the distribution coefficient (K_d) [L/g] were calculated from the difference between the initial and equilibrium concentrations from the equations:

$$q_e = \left(C_0 - C_e\right) \times \frac{V}{m} \tag{1}$$

$$\%S = \frac{C_0 - C_t}{C_0} \times 100\% \tag{2}$$

$$K_d = \frac{\left(C_0 - C_t\right)}{C_t} \times \frac{V}{m} \tag{3}$$

where: C_0 is the initial *U* (VI) concentration [mg/L], C_{eq} is the *U* (VI) equilibrium concentration [mg/L], *m* is the sorbent mass [g], *V* is the volume of the solution [L].

Results and discussion

XRD

The white clay sample is crystalline and the nanocomposite is crystalline too containing both crystalline phases. The crystalline structure was analyzed using the XRD method recording patterns at 2q = 10–80°. Comparison of the obtained patterns with the ASTM database shows that hydroxyapatites are crystalline in individual HAPs (the peaks characteristic of the crystalline form of HAP are evidenced by the following 2q values and the corresponding intensities: 25.9–100%, 32.96–55%, 39.84–20%; 46.7–40% and 49.5–30%), as well white clay as crystallite kaolinite $Al_4(OH)_8Si_4O_{10}$ with the admixtures of quartz and illite. The nanocomposite has the peaks characteristic of hydroxyapatite, kaolinite and apatite. Such structure of the nanocomposite can promote some applications as a biomaterial (Broda et al. 2019).

As follows from the XRD analysis after U(VI) adsorption on the HAP surface, there is formed a new compound calcium uranyl phosphate hydrate $Ca(UO_2)_2(PO_4)_2(H_2O)_{11}$ on the surface in the amount of 69% but 31% is nano-hydroxyapatite. The XRD studies after U (VI) adsorption did not show a new crystalline form on the surface of white clay or HAP/ white clay, only some differences in the crystallite size were detected by the Scherrer method. The size of crystallites computed using the Scherrer method was HAP = 24 nm; white clay = 38 nm; HAP/white clay = 21 nm; HAP/U (VI) = 18 nm; white clay /U (VI) = 26 nm white clay/HAP/U (VI) = 17 nm. This correlates well with the results of adsorption described later, and confirms the possibility of using the nanocomposite for the removal of 6-valued uranium from aqueous solutions.

ASAP

According to the data in Table 1, it can be concluded that the surface area of the synthesized Hap/clay nanocomposite is larger than surface area of hydroxyapatite or clay independently. It can improve its adsorption ability. The nanocomposite as well as Hap or pure clay is mesoporous, however, the size of pores is larger in the case of the nanocomposite. Adsorption of *U* (VI) ions results in the decreasing surface area and pore size for the Hap and Hap/clay nanocomposite. The influence of adsorption on the clay surface area and pore size is not significant, it can be an effect of small surface area of the material used in the nanocomposite synthesis and numerous mesopores on the surface.

The measurements were made after samples degassing at the reduced pressure, and the results are shown in Table 1. Following on the results (Table 1), *U* (VI) adsorbed on the surface causes significant decreases in the specific surface area and decrease in the average radius of the pores which may be due to formation of the calcium uranyl phosphate hydrate layer on the nano-hydroxyapatite layer as confirmed by the XRD studies. The specific surface area decreases also after the *U* (VI) adsorption for the systems: HAP/white clay and white clay (Table 1). The volume of pores increases (Table 1) which may be due to formation of $CaCO_3$ that results in Ca ions escape from the surface of hydroxyapatite causing a simultaneous pore volume increase. The amount of Ca ions is the largest on the surface in the hydroxyapatite structure compared to the other elements building it.

The dependence of the pore size distribution on the pore volume was also prepared Fig. 2. On the basis of these results, we can say that in the tested solids there are: micropores, mesopores and macropores. Mesoporous are the most numerous and they have a dominant influence on the structure of the surface area. One can also notice a decrease in the pore volume due to the adsorption of *U* (VI) ions on the tested solids.

Table 1 Surface characteristics of HAP, Hap/white clay nanocomposite and white clay—comparison of the properties before and after the adsorption of uranyl ions

	HAP	HAP/U(VI)	HAP/white clay	HAP/white clay/*U*(VI)	White clay	White clay/*U*(VI)
BET surface area [m^2/g]	55	25	63	34	18	19
Langmuir surface area [m^2/g]	80	37	92	50	25	28
BJH cumulative adsorption surface area of pores from 1.7 nm to 300 nm diameter [cm^3/g]	0.32	0.13	0.29	0.17	0.09	0.11
BJH cumulative desorption surface area of pores from 1.7 nm to 300 nm diameter [cm^3/g]	0.32	0.13	0.30	0.17	0.09	0.11
Average pore diameter (4 V/A by BET) [nm]	23.50	20.36	28.69	20.42	20.94	22.81
BJH adsorption on the average pore diameter[nm]	24.44	20.75	29.48	20.95	22.81	21.97
BJH desorption on the average pore diameter (4 V/A) [nm]	22.93	13.51	26.99	16.21	21.13	20.03
Micropore area[m^2/g]	6.54	3.54	5.65	3.71	1.50	1.18
Micropore volume [cm^3/g]	0.003	0.002	0.002	0.001	0.0005	0.0004
Total pore volume [cm^3/g]	0.33	0.13	0.29	0.17	0.09	0.11
V_{mic}/V_t	0.009	0.02	0.007	0.006	0.006	0.004

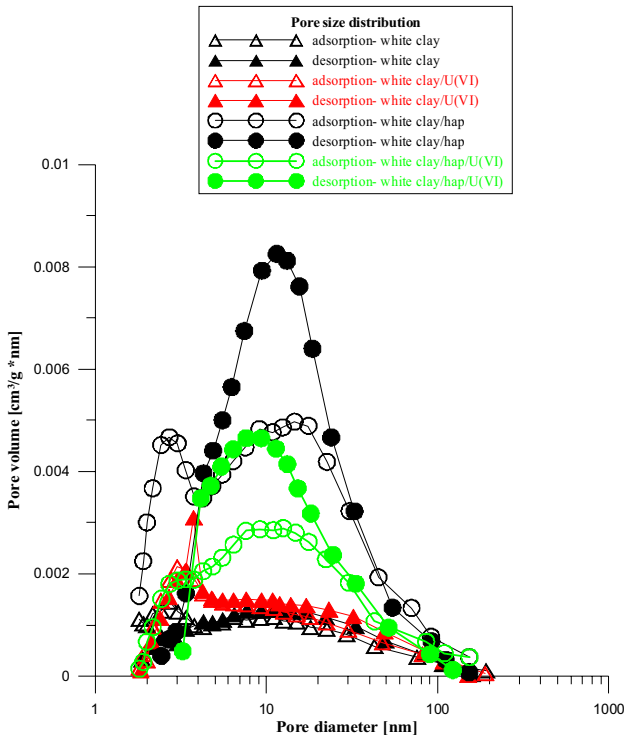

Fig. 2 Pore size distribution for adsorbents

XRF

The XRF analysis was performed for the pure clay and Hap/white clay nanocomposite. The XRF results confirmed the uranium adsorption. After the uranium adsorption pure clay contains 1.6% of uranium, whereas Hap/white clay nanocomposite 9.1% of uranium. This shows that the nanocomposite is a better adsorbent of uranium than the pure clay.

Table 2 Diameter size of grains in time

	0 h [nm]	3 h [nm]	48 h [nm]	7 days [nm]
Hap/$NaNO_3$	2638	2412	2345	2529
White clay/$NaNO_3$	3930	6474	7731	7815
Hap/White clay/$NaNO_3$	7636	7844	7866	8673
Hap/$NaNO_3$/U	4524	7312	8031	8321
White clay/$NaNO_3$/U	5287	6475	6899	6979
Hap/white clay/$NaNO_3$/U	6980	9998	10,939	9366

Analysis of particle distribution

Table 2 shows the diameters of grains for the Hap, clay and Hap/white clay nanocomposite. The test was repeated at different periods of time. After 3 h the average radius of the particle increases. Later the increment is smaller. This may be due to particles agglomeration.

Electrokinetic measurements

According to the Smoluchowski theory, there is a linear relationship between the electrophoretic mobility U_e and the ζ potential: $U_e = A\zeta$. where A is the constant for a thin electrical double layer (EDL) at $\kappa a \gg 1$ (where a denotes the particle radius and κ is the Debye–Huckel parameter). For a thick EDL ($\kappa a < 1$), e.g., at pH close to the isoelectric point (IEP), the equation with the Henry correction factor is more appropriate $U_e = 2\varepsilon\zeta/(3\eta)$, where ε is the dielectric permittivity; and η is the viscosity of the liquid.

The surface charge density was calculated using the potentiometric titration data for a blank electrolyte solution and oxide suspensions ($C_{ox} = 0.2$ wt.% for all oxides),

at the constant salinity of 10^{-3} mol/dm^3 $NaNO_3$. From the difference of acid or base volume utilized to obtain the same pH value as that for the background electrolyte of the same ionic strength according to the following equation, one can calculate the surface charge density $\sigma = \Delta VcFmS_{BET}$, where $\Delta V = V_s - V_e$ is the difference between the base (acid) volumes added to the electrolyte solution V_e and the suspension V_s to achieve the same pH; F is the Faraday constant, c is the concentration of base (acid) and m is the weight of the adsorbents.

The structure of interfacial water can be also characterized by the ζ potential as a function of pH and the surface charge density. Notice that the ζ potential and the surface charge density deal with different planes (i.e. shear and surface planes, respectively).

The difference in the surface composition of the clay, hydroxyapatite (Hap) and clay/Hap nanocomposite samples causes noticeable differences in their behaviour in the aqueous media (Figs. 3, 5, 6, 7), especially for clay/Hap in comparison with clay and hydroxyapatite samples because of the specific surface area of clay/Hap sample (Table 1). This results in the different function as well as of the ζ(pH) potential and σ_0(pH) can lead to complex pH dependences of other properties of the clay/Hap dispersions, such as aggregation of particles, adsorption of dissolved compounds and metal ions, suspension viscosity, the thickening ability, etc.

Consequently, the parallel analysis of the surface composition and the adsorption of U(VI) ions allows more profound insight into their adsorption mechanisms.

Figures 3, 4 and 5 include the comparison of the surface charge density for the Hap, white clay and their nanocomposite in the solution containing different concentrations of U (VI) ions. The charts show the decrease of surface charge density for the Hap and pure clay while the pH increase (but the absolute value of the surface charge density increases). The influence of pH on the surface charge density for Hap/white clay nanocomposite is not significant. In most cases the nanocomposite is characterized by the lower absolute value of surface charge density. The assay of U (VI) ions impacts profoundly on Hap.

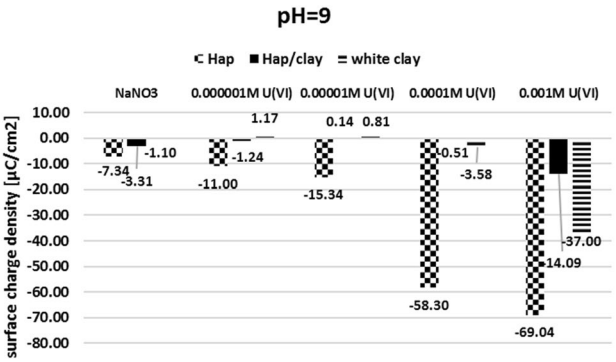

Fig. 4 Comparison of the surface charge density for the hydroxyapatite, Hap/white clay nanocomposite and white clay dispersed in 0.001 mol/dm^3 sodium nitrate with different concentrations of uranyl nitrate at pH = 9

Table 3 presents the determined values of pH_{pzc} at the Hap/electrolyte, clay/electrolyte and Hap/clay/electrolyte nanocomposite interface, estimated by the method of the addition of different weights of the given adsorbent white the electrolyte concentration remains stable. The higher value of pH_{pzc} in the electrolyte without the addition of U (VI) ions is observed for white clay, the lowest value—for Hap, whereas Hap/white clay nanocomposite exhibit intermediate pH_{pzc}. The obtained results for white clay and Hap are consistent with literature data. (Kosmulski 2001).

In Figs. 6, 7, 8, 9, zeta potential for the Hap, clay and Hap/clay nanocomposite are graphed. It can be observed that when pH of the suspension increases, the zeta potential value decreases. The value of zeta potential of nanocomposite usually has a medium level of the zeta potential for the

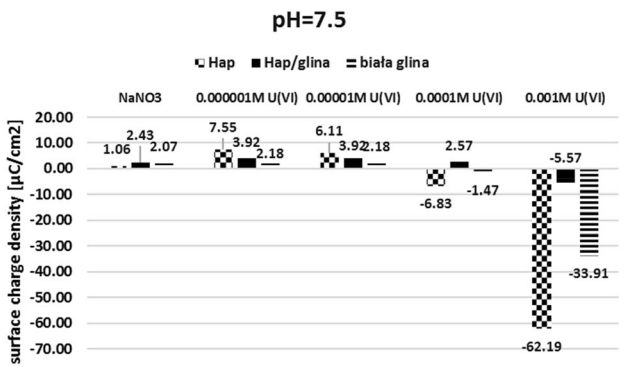

Fig. 3 Comparison of the surface charge density for the hydroxyapatite, Hap/white clay nanocomposite and white clay dispersed in 0.001 mol/dm^3 sodium nitrate with different concentrations of uranyl nitrate at pH = 7.5

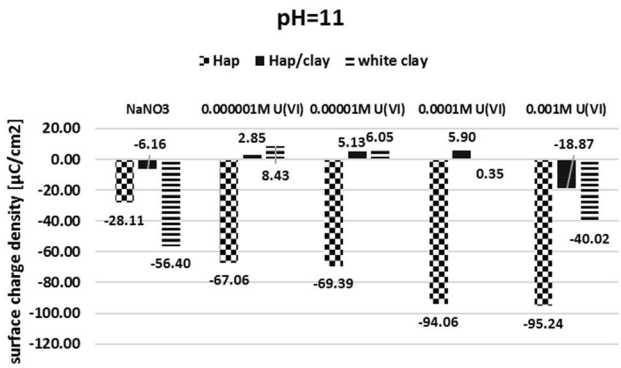

Fig. 5 Comparison of the surface charge density for the hydroxyapatite, Hap/white clay nanocomposite and white clay dispersed in 0.001 mol/dm3 sodium nitrate with different concentrations of uranyl nitrate at pH = 11

Table 3 Determined values of pH_{pzc} and pH_{IEP}

Sample	pH_{pzc}					pH_{IEP}
	Concentration of U(VI)					
	0	0.000001 M	0.00001 M	0.00001 M	0.001 M	0
Hap	7.9	8.1	7.9	7.3	5.6	< 4
Hap/clay Nanocomposite	9.0	9.1	8.7	8.6	6.8	< 2
White clay	9.7	10.4	9.6	6.4	4.2	< 2

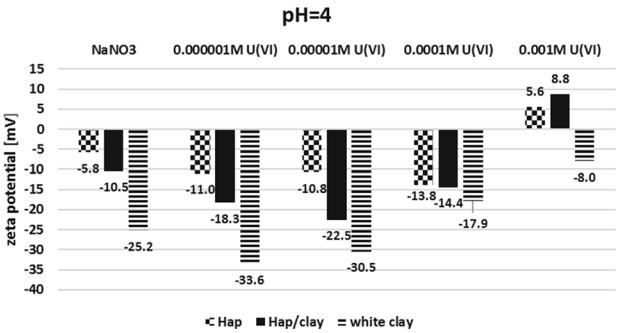

Fig. 6 Comparison of the zeta potential for the hydroxyapatite, Hap/white clay nanocomposite and white clay dispersed in 0.001 mol/dm3 sodium nitrate with different concentrations of uranyl nitrate at pH = 4

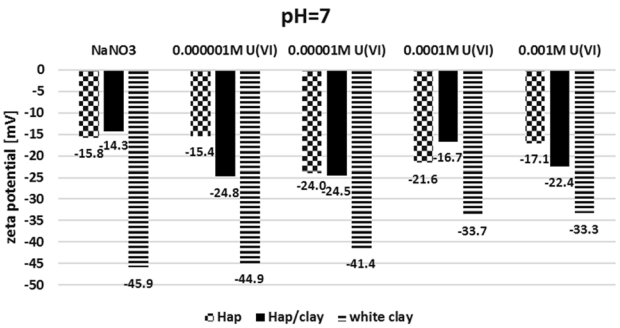

Fig. 7 Comparison of the zeta potential for the hydroxyapatite, Hap/white clay nanocomposite and white clay dispersed in 0.001 mol/dm^3 sodium nitrate with different concentrations of uranyl nitrate at pH = 7

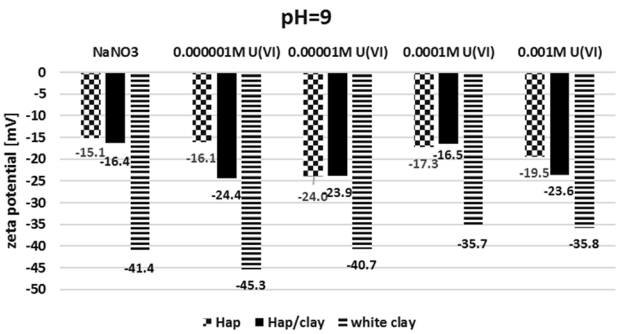

Fig. 8 Comparison of the zeta potential for the hydroxyapatite, Hap/white clay nanocomposite and white clay dispersed in 0.001 mol/dm^3 sodium nitrate with different concentrations of uranyl nitrate at pH = 9

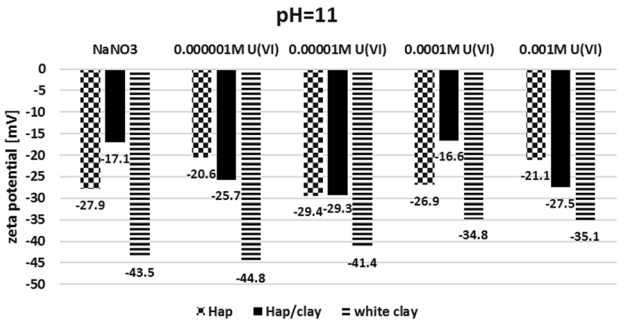

Fig. 9 Comparison of the zeta potential for the hydroxyapatite, Hap/white clay nanocomposite and white clay dispersed in 0.001 mol/dm^3 sodium nitrate with different concentrations of uranyl nitrate at pH = 11

given system (fixed pH and concentration of *U* (VI) ions). The value of the zeta potential for the pure clay and chosen systems of Hap reaches the level of < − 30 mV. Under such condition the suspension is electrolytically stable. The synthesized Hap/white clay nanocomposite creates a less stable colloid system than each of its component independently.

Adsorption

Effect of time

The effect of time on uranium adsorption on the white clay and Hap/white clay nanocomposite is shown in Fig. 10. As can be seen the percentage of uranium removal by both tested sorbents was significant during 0–120 min with a linear slope. After this time, the uranium adsorption has got stabilized which may be due to the saturation of adsorption sites on the surface of adsorbents and an increase in the resistance to diffusion of free ions to the inner surface. Equilibrium was achieved after 180 min with 78% removal for the white clay and 100% for the Hap/white clay nanocomposite.

Isotherm of adsorption

In order to determine the maximum adsorption capacity, the influence of the initial concentration of U(VI) ions on the course of the sorption process on two white clay-based

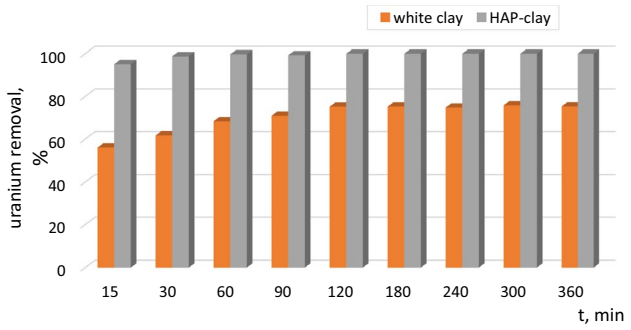

Fig. 10 Removal of uranium by the white clay and Hap/white clay nanocomposite at different adsorption times (c_{in} = 119 mg/L, pH = 5, T 295 K)

adsorbents was investigated. A series of solutions with uranyl ion concentrations ranging from 0.1 to 1 mg/L were prepared and 50 mL of relevant solution was contacted with 50 mg of the adsorbent. The results are presented in Fig. 11. The most common adsorption isotherms: Freundlich, Langmuir–Freundlich and Dubinin–Radushkevich were used to describe the interactions between the uranyl ions and the above-mentioned adsorbents to fit the experimental data.

The Freundlich isotherm equation: $Q = K_F \cdot c_{eq}^{1/n}$;

the Langmuir–Freundlich isotherm equation:$Q = A\left(K_L \cdot c_{eq}\right)^n / \left[1 + \left(K_L \cdot c_{eq}\right)^n\right]$;

the Dubinin–Radushkevich isotherm equation: $Q = q \cdot \exp(-K_{D-R}\varepsilon^2)$, where Q is the adsorption capacity (mg/g), A is the Langmuir monolayer sorption capacity (mg/g), K is the constant (L/mg), ε is the Polanyi potential, n is the constant.

The parameters of these isotherms were calculated from the linearized plots, Ceq vs. Q. The Langmuir–Freundlich isotherm model predicts the formation of an adsorbate monolayer on a homogeneous adsorbent surface and the participation of side interactions between the adsorbed ions. The Freundlich model takes a different approach, does not predict surface saturation and considers the existence of a multi-layer structure. The calculated parameters of the isotherm for the U(VI) sorbent systems are presented in Table 4. The correlation coefficients R^2 of the Freundlich model (R^2 = 0.76–0.79) were slightly lower than in the Langmuir–Freundlich model (R^2 = 0.94–0.99) for the white clay systems and higher (0.95–0.98) for the Hap/white clay nanocomposite sorbent. 1/n values were in the range of 0.118–0.588 for both adsorbents, indicating preferential adsorption of uranyl ions. The Langmuir–Freundlich isotherm is often used to quantify different adsorbents. The monolayer adsorption capacity was in the range of 7.88–12.73 mg/g (R^2 = 0.934–0.998) in the case of white clay. The highest Q value was found for the Hap/white clay nanocomposite adsorbent (570–670 mg/g). The mean energy of sorption, E, is the free energy change when one mole of ion is sorbed on the solid surface from the solution, calculated from: $E = (-2\ \mathrm{K})^{-1/2}$. The value of the sorption energy was found to be 7–9.8 kJ/mol which is within the energy range for chemisorption (Gładysz-Płaska et al. 2018a, b).

Effect of temperature

The influence of temperature on adsorption ranging from 295 to 333 K was investigated. Figure 12 shows that the amount of uranium adsorbed by the white clay and Hap/white clay nanocomposite gradually increased with the increasing temperature. At the temperature higher than 320 K, a plateau is observed on the graph, which proves that further temperature increase will not increase the adsorption significantly. The dependence of the adsorption efficiency on the temperature is justified by the fact that we are dealing here with a chemisorption reaction in which the binding forces are greater than the van der Waals forces. Therefore, it is necessary to provide the system

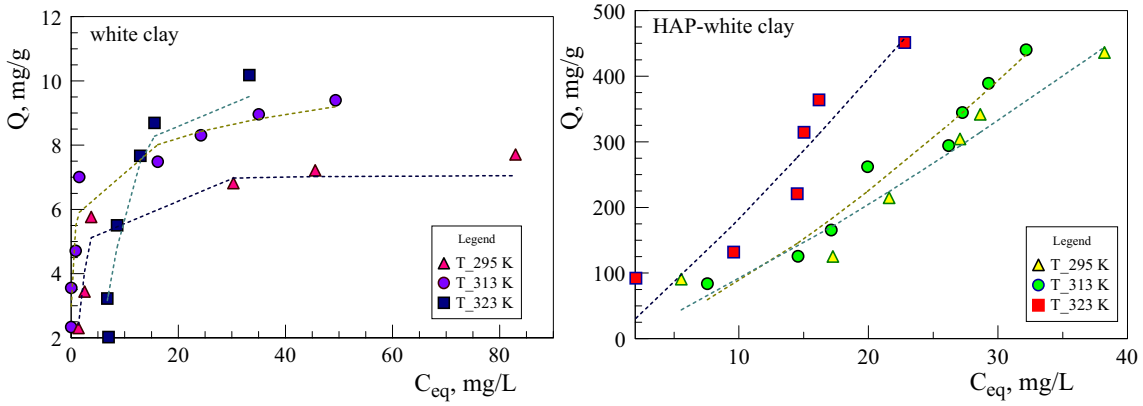

Fig. 11 Adsorption isotherms of uranium removal on the white clay and Hap/white clay nanocomposite at different temperatures (295, 313, 323 K); pH = 5

Table 4 Fitting parameters of the isothermal adsorption models for uranium adsorption on the white clay and HAP/white clay nanocomposite

White clay			
Model	295 K	313 K	323 K
Freundlich	18.91	25.82	28.21
K, L/mg	0.418	0.399	0.588
1/n	0.783	0.788	0.761
R^2			
Langmuir–Freundlich	7.88	10.09	12.73
A, mg/g	0.563	7.243	18.72
K, L/mg	0.52	0.6	0.88
n	0.998	0.986	0.934
R^2			
Dubin–Radushkevich	8.9	8.8	9.5
Q, mg/g	9.81	9.44	8.20
E, kJ/mol	0.958	0.906	0.856
R^2			
Hap/white clay Nanocomposite			
Model	295 K	313 K	323 K
Freundlich	89.61	41.49	36.78
K, L/mg	0.371	0.117	0.197
1/*n*	0.956	0.966	0.971
R^2			
Langmuir–Freundlich	570.8	641.2	669.9
A, mg/g	25.18	92.99	122.67
K, L/mg	0.715	0.679	0.469
n	0.899	0.887	0.888
R^2			
Dubin–Radushkevich	574.2	416.4	513.6
Q, mg/g	7.51	7.55	9.49
E, kJ/mol	0.968	0.882	0.913
R^2			

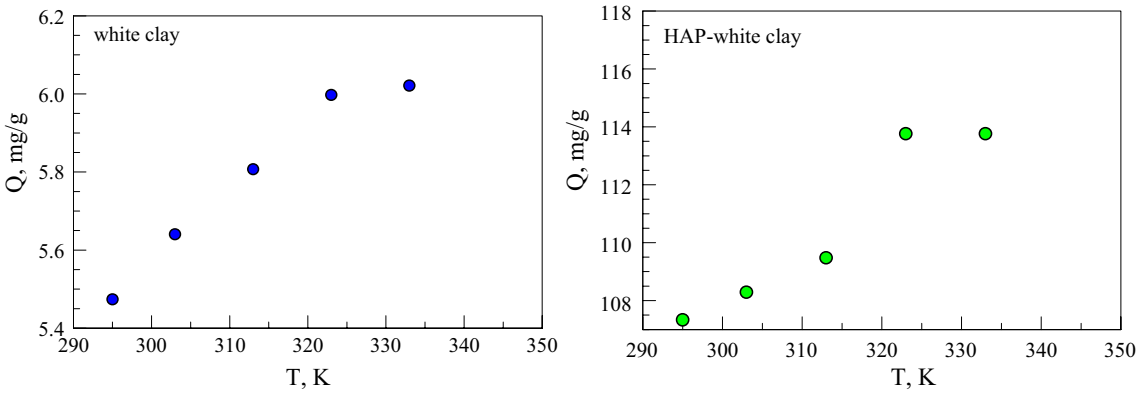

Fig. 12 Effect of temperature on uranium adsorption on white clay and Hap/white clay nanocomposite (c_{in} = 119 mg/L, pH = 5)

with the appropriate energy needed to cross the energy barrier of chemisorption [Li et al. 2018, Yang et al. 2017].

The thermodynamic parameters presented in Table 5 were calculated based on of the following formulas:

$$K = Q/c_{eq}$$

$$\Delta G = -RT\ln K$$

Table 5 Thermodynamic parameters of uranium adsorption on the white clay and Hap/white clay nanocomposite at different temperatures

Temperature, K	White clay				Hap/white clay Nanocomposite			
	K, L/mol	Δ*G*, kJ/mol	Δ*H*, kJ/mol	Δ*S*, kJ mol^{-1} K^{-1}	K, L/mol	Δ*G*, kJ/mol	Δ*H*, kJ/mol	Δ*S*, kJ mol^{-1} K^{-1}
295	4.82	− 3.86	7.59	26.03	9.21	− 5.44	26.54	90.1
303	4.97	− 4.04	7.78		10.11	− 5.83	27.93	
313	5.13	− 4.25	8.19		11.51	− 6.36	28.46	
323	5.31	− 4.45	8.32		21.72	− 8.27	29.37	
333	5.32	− 4.66	8.37		21.73	− 8.52	29.62	

$$\Delta G = \Delta H - T\Delta S$$

where K is the distribution coefficient, R is the universal gas constant (8.314 J mol^{-1} K^{-1}), T is the temperature (K), ΔG is the Gibbs free energy (kJ/mol), ΔH is the enthalpy (kJ/mol) and ΔS is the entropy (kJ mol^{-1} K^{-1}).

There were negative ΔG values, which prove that the adsorption of uranium on the tested adsorbents was possible and spontaneous. The positive ΔH values suggest the endothermic nature of adsorption, while the positive ΔS values indicate an increase in randomness at the solid—solution interface during the adsorption process.

The effect of pH

Due to the surface properties of adsorbents, one of the factors taken into account when assessing its adsorption capacity is pH (Fig. 13). Its influence is related to the influence on the chemical behaviour of the adsorbent as well as the adsorbate, i.e. species forms present in solutions at different pH values and the nature of the structures formed between the adsorbate and the adsorbent. As follows from the literature on the speciation of uranyl ions, the dominant species are: UO_2^{2+} at pH < 5. The uranyl ions undergo hydrolysis, polymerization and complexation reactions with the increasing pH with the formation of multi-core hydroxycomplexes in the solution, e.g. as UO_2OH^+, $UO_2(OH)_3^-$. The increase in the uranyl sorption above pH > 4 coincides with a significant increase in the concentration of UO_2OH^+ and UO_2^{2+} species are still present in the solution at pH 4–6 and 6–8, respectively. At pH > 8.5 the uranium sorption decreases, reflecting uranium complexation on the hydroxyapatite surface. Hydronium H_3O^+ ions compete for active sites on the sorbent surface for metal cations, especially at a low pH of the solution, therefore usually low adsorption is observed in this range. As the pH increases, the adsorption of metal ions increases as the number of hydronium ions decreases and it is the highest in the range of approximately pH = 4. This is due to the fact that the sorbent surface becomes negatively charged as a result of the deprotonation reaction [Thakur et al. 2005, Skwarek et al. 2019, Gładysz-Płaska 2019]. Accordingly, the repulsive force that exists between the metal ions in the solution and the active groups of sorbents is reduced, thereby increasing the removal of metal ions from the solution. Therefore, the mechanism of uranyl ion sorption is largely based on the ion exchange process between the exchangeable protons from the sorbent hydroxyl groups and the UO_2^{2+} cations. This is confirmed by the fact that the equilibrium pH of the solutions is lowered compared to the initial pH. This mechanism plays a decisive role in the adsorption of uranyl ions on the white clay. The highest adsorption, close to 110 mg/g, was found for the Hap/

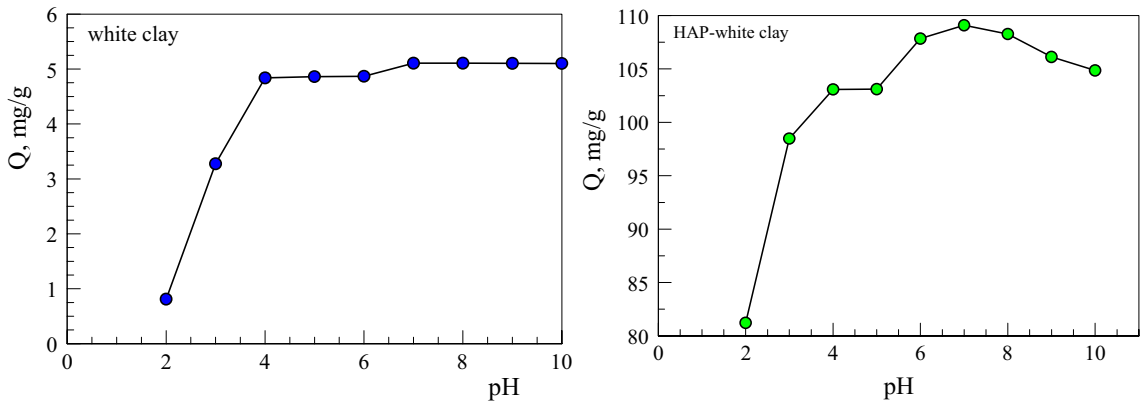

Fig. 13 Effect of pH on uranium adsorption on the white clay and Hap/white clay nanocomposite (c_{in} = 119 mg/L)

white clay nanocomposite sorbent, in the case of which from pH = 4 to pH = 10, there was a plateau at the level of 100% adsorption. In this pH range, there is the precipitation of $H_2(UO_2)_2(PO_4)_2 \cdot 10\ H_2O$ sediment on the adsorbent surface which results in the high adsorption value.

Conclusion

In this study the nanocomposite of white clay and hydroxyapatite was obtained by wet method. The surface properties were tested by the low-temperature nitrogen adsorption–desorption method (ASAP) and XRD method. Based on the XRD results the white clay and hydroxyapatite phases can be distinguished in the diffractogram of Hap/white clay nanocomposite. The surface analysis by ASAP demonstrates that the nanocomposite has the structural properties intermediate between pure clay and Hap. After the adsorption of U (VI) decreasing surface area can be observed in the case of the Hap and Hap/white clay nanocomposite. However, no relevant change is noticed in case of pure clay.

This can be caused by adsorption of U (VI) on the surface of tested adsorbents. Adsorption of uranyl ions was tested on the Hap/white clay nanocomposite and white clay separately. Both systems reached the equilibrium after 180 min. The adsorption capacity proved to be higher for nanocomposite than for pure clay. Hap/white clay nanocomposite can be promising adsorbent applied for wastewater management. The mechanism of uranyl ion sorption is largely based on the ion exchange process between the exchangeable protons from the sorbent hydroxyl groups and the UO_2^{2+} cations.

Funding The financial support from the National Science Centre (Poland) within project Miniatura 1 No.2017/01/X/ST4/01939 is acknowledged.

Declarations

Conflict of interest On behalf of all authors, I state that there is no conflict of interests.

References

Aly MM, Hamza MF (2013) A review: studies on uranium removal using different techniques. Overview J Disper Sci Tech 34(2):182–213

Bachmaf S, Merkel B (2011) Sorption of uranium (VI) at the clay mineral–water interface. Environ Earth Sci 63:925–934

Bleise A, Danesi PR, Burkart W (2003) Properties, use and health effects of depleted uranium (DU): a general overview. J Environ Radioact 64:93–112

Broda E, Skwarek E, Payentko VV, Gunko VM (2019) Synthesis and selected physicochemical properties of hydroxyapatite and white clay composite. Physicochem Probl Miner Process 55(6):1475–1483

Ersan M, Guler UA, Acikel U, Sarioglu M (2015) Synthesis of hydroxyapatite/clay and hydroxyapatite/pumice composites for tetracycline removal from aqueous solutions. Process Saf Environ Prot 96:22–32

Fijałkowska G, Wiśniewska M, Szewczuk-Karpisz K (2020) Adsorption and electrokinetic studies in kaolinite/anionic polyacrylamide/chromate ions system. Colloids Surf A 603:125232

Gładysz-Płaska A (2019) Adsorption properties of sepiolite in relation to uranium and lanthanide ions. Minerals 9:686–702

Gładysz-Płaska A, Grabias E, Majdan M (2018a) Simultaneous adsorption of uranium(VI) and phosphate on red clay. Progress Nucl Energy 104:150–159

Gładysz-Płaska A, Majdan M, Tarasiuk B, Sternik D, Grabias E (2018b) The use of halloysite functionalized with isothiouronium salts as an organic/inorganic hybrid adsorbent for uranium(VI) ions removal. J Hazard Mater 354:133–144

Hokkanen S, Bhatnagar A, Srivastava V, Suorsa V, Sillanpää M (2018) Removal of Cd^{2+}, Ni^{2+} and from aqueous solution by hydroxyapatite–bentonite clay–nanocellulose composite. Inter J Biol Macromole 118:903–912

Katsoyaiannis IA, Zouboulis AI (2013) Removal of uranium from contaminated drinking water: a mini review of available treatment methods. Desalin Water Treat 51(13–15):2915–2925

Keith LS, Faroon OM, Fowler BA (2007) Handbook on the toxicology of metals (Third Edition). In: Nordberg GF, Fowler BA, Nordberg M, Friberg LT (eds) Uranium, 3rd edn. Academic Press, Cambridge, pp 881–903

Kosmulski M (2001) Technical properties of material surfaces. Surfactant science series, vol 102. Marcel Dekker, New York

Li J, Li X, Alsaedi A, Hayat T, Chen C (2018) Synthesis of highly porous inorganic adsorbents derived from metal–organic frameworks and their application in efficient elimination of mercury(II). J Colloid Interface Sci 517:61–71

Marczenko Z, Balcerzak M (1998) Spectrophotometric methods in inorganic analysis. PWN SA, Warsaw

Shi Q, Su M, Yuvaraja G, Tang J, Kong L, Chen D (2020) Development of highly efficient bundle-like hydroxyapatite towards abatement of aqueous U(VI) ions: Mechanism and economic assessment. J Hazard Mater. https://doi.org/10.1016/j.jhazmat.2020.122550

Skwarek E, Gładysz-Płaska A, Choromańska JB, Broda E (2019) Adsorption of uranium ions on nano-hydroxyapatite and modified by Ca and Ag ions. Adsorption 25:639–647

Szewczuk-Karpisz K, Fijałkowska G, Wiśniewska M, Wójcik G (2020) Chromium(VI) reduction and accumulation on the kaolinite surface in the presence of cationic soil flocculant. J Soils Sedim 20:3688–3697

Thakur P, Moore RC, Choppin GR (2005) Sorption of U(VI) species on hydroxyapatite. Radiochim Acta 93:385–391

Wiśniewska M, Fijałkowska G, Szewczuk-Karpisz K (2018) The mechanism of anionic polyacrylamide adsorption on the

montmorillonite surface in the presence of Cr(VI) ions. Chemosphere 211:524–534
Yang M, Junfeng KE, Xiaoman HE, Lei N, Zhang Q (2017) Adsorption of Cu(21) in aqueous solution by sodium hydroxide modified zeolite. Environ Pollut Control 39:314–318
Zhu B, Ryan D (2018) Complexation study of uranyl ion with dissolved organic matter in natural freshwater by fluorescence quenching techniques. IntechOpen. https://doi.org/10.5772/intechopen.72861